Key Points:
- We compile a global digital database of seismic anisotropy observations in the D′′ layer
- We compute the global ray coverage of different methods used to detect deep mantle anisotropy
- In the context of a global compilation, there is no preferential occurrence of seismic anisotropy at large-low velocity province edges

Correspondence to:
J. Wolf,
jonathan.wolf@yale.edu

Global Compilation of Deep Mantle Anisotropy Observations and Possible Correlation With Low Velocity Provinces

Jonathan Wolf[1] , Maureen D. Long[1] , Mingming Li[2] , and Edward Garnero[2]

[1]Department of Earth and Planetary Sciences, Yale University, New Haven, CT, USA, [2]School of Earth and Space Exploration, Arizona State University, Tempe, AZ, USA

Abstract We compile and make publicly available a global digital database of body wave observations of seismic anisotropy in the D′′ layer, grouped using the method used to analyze deep mantle anisotropy. Using this database, we examine the global distribution of seismic anisotropy in the D′′ layer, evaluating the question of whether seismic anisotropy is more likely to be located at the edges of the two large-low velocity provinces (LLVPs) in Earth's mantle than elsewhere. We show that this hypothesis lacks statistical justification if we consider previously observed lowermost mantle anisotropy, although there are multiple factors that are difficult to account for quantitatively. One such factor is the global lowermost mantle ray coverage for different phases that are commonly used to detect deep mantle anisotropy in shear wave splitting studies. We find that the global ray coverage of the relevant seismic phases is highly uneven, with LLVP edges and their interiors less well-sampled than the global average.

Plain Language Summary Seismic waves caused by earthquakes sometimes travel at different speeds in different directions. This material property, called seismic anisotropy, indicates convective flow and deformation in the mantle and has been detected in the lowermost mantle. We compile a database of lowermost mantle anisotropy locations from the previously published literature. Previous studies have reported strong seismic anisotropy at the edges of large features with lower than average seismic velocities in Earth's mantle, called large-low velocity provinces. Here, we test whether seismic anisotropy is also more likely at large-low velocity province edges than elsewhere. Our statistical analysis of our database suggests that this may not be the case. This analysis, however, did not explicitly account for the fact that the number of seismic waves traveling through the lowermost mantle is different from region to region.

1. Introduction

Seismic anisotropy, or the directional dependence of seismic wave speed, has been detected at a range of depths in the Earth. For example, the crust (e.g., Barruol & Kern, 1996; Erdman et al., 2013) and the upper mantle (e.g., Savage, 1999; Silver, 1996; Zhu et al., 2020) are anisotropic in many regions. While the bulk of the lower mantle appears largely isotropic (e.g., Chang et al., 2015; Panning & Romanowicz, 2006), seismic anisotropy has been found in the lowermost 200–300 km of the mantle (e.g., Asplet et al., 2023; Lay et al., 1998; Nowacki et al., 2010; Wolf & Long, 2022; Wookey et al., 2005), known as the D′′ layer. Seismic anisotropy can be induced by deformation and alignment of minerals due to mantle convection. Thus, observations of seismic anisotropy are helpful to infer dynamic processes in Earth's interior (e.g., Long & Becker, 2010). Seismic anisotropy can be detected through the analysis of shear waves, specifically how they split into fast and slow components in the presence of anisotropy (e.g., Long & Silver, 2009).

Through analyses of deep mantle anisotropy, better knowledge about flow patterns at the base of the mantle can be obtained, potentially elucidating several big-picture aspects of mantle dynamics, such as the origin and evolution of large-low velocity provinces (LLVPs), the fate of subducted slabs, and core-mantle boundary (CMB) heat flow (e.g., Bercovici & Karato, 2003; Hernlund et al., 2005; Wenk & Romanowicz, 2017; Wolf & Evans, 2022). Based on several previous regional studies (e.g., Cottaar & Romanowicz, 2013; Deng et al., 2017; Lynner & Long, 2014; Reiss et al., 2019; Wang & Wen, 2004), it has been suggested that lowermost mantle anisotropy is particularly strong, and thus easily observable, near LLVP edges (e.g., Reiss et al., 2019; Wenk & Romanowicz, 2017). This may reflect strong deformation, perhaps due to mantle flow impinging on their sides (e.g., Li & Zhong, 2017; McNamara et al., 2010), or due to the generation of mantle plumes at LLVP edges (e.g., Li & Zhong, 2017; Steinberger & Torsvik, 2012). Subducting slabs likely represent one of the main drivers of

flow and deformation at the base of the mantle (e.g., Bercovici & Karato, 2003; Chandler et al., 2021; McNamara et al., 2002; Tackley, 2000), and several studies have identified seismic anisotropy associated with slab remnants at the base of the mantle (e.g., Long, 2009; Nowacki et al., 2010; Wolf & Long, 2022), in locations away from LLVP edges. More observations, with increased resolution of anisotropic regions of the lowermost mantle, will continue to shed light on the patterns and drivers of flow in the deepest mantle, the interactions among different deep mantle structures (e.g., LLVPs, hotspots, ULVZs, and subducted paleoslabs), and their respective roles in deep mantle dynamics and evolution.

In this study, we compile a global digital database of seismic anisotropy locations in the D″ layer that have been detected to date (Table 1; Figure 1). We make this database openly available on GitHub (https://github.com/wolfjonathan/Deep_Mantle_Anisotropy_Database) and in a data repository (Wolf et al., 2023c), in the hope that it will enable future investigations of D″ anisotropy in the context of deep mantle composition and dynamics. We use these global data set to investigate whether there is a statistical spatial correlation between D″ anisotropy locations and edges of LLVPs, as has been suggested previously (e.g., Wenk & Romanowicz, 2017).

2. Strategies to Analyze Deep Mantle Anisotropy

D″ anisotropy has been explored with different strategies using a variety of seismic body wave phases (Figure 2). These splitting methods have been refined over time, and their strengths and weaknesses were explored and different pitfalls were pointed out. We distinguish between these different methods in our database (Table 1; Figure 2). The increasing availability of computing resources enables detailed assessments of existing methods to analyze deep mantle anisotropy as well as the development of new strategies (e.g., Komatitsch et al., 2010; Nowacki & Wookey, 2016; Parisi et al., 2018; Wolf et al., 2022a, 2022b, 2023b).

Many early studies measured differential SV-SH travel times from teleseismic S, ScS and S_{diff} waves (Figure 2a), which are interpreted as being due to D″ anisotropy (e.g., Kendall & Silver, 1998; Pulliam & Sen, 1998; Rokosky et al., 2004). Recent studies, however, have demonstrated that under some circumstances, differential SV-SH travel times can also be caused by isotropic structure (e.g., Borgeaud et al., 2016; Komatitsch et al., 2010; Parisi et al., 2018) for waves that are initially polarized to have both SV and SH energy. Therefore, it is unclear to what extent previously reported SV-SH differential times conclusively require deep mantle anisotropy.

Additionally, measurements of polarities of S phases that turn in the lowermost mantle (Figure 2b) have been used to infer deep mantle anisotropy (e.g., Garnero, Maupin, et al., 2004; Maupin et al., 2005). Later studies expanded polarity analyses to consider D″-reflected SdS and PdP waves (Figure 2b; e.g., Pisconti et al., 2019; Thomas et al., 2011). Some of these studies show that changes in polarity are likely caused by the presence of seismic anisotropy (e.g., Garnero, Maupin, et al., 2004; Maupin et al., 2005), and others use polarities of reflected waves as an additional constraint on the nature of an anisotropic D″ region along with a different method (Pisconti et al., 2019, 2023).

Wang and Wen (2004) and Niu and Perez (2004) were among the first studies to interpret differences in SKS and SKKS splitting in terms of deep mantle anisotropy. This technique became increasingly useful when applied to larger data sets (e.g., Deng et al., 2017; Long, 2009). The SKS-SKKS differential splitting technique relies on the argument that the raypaths of SKS and SKKS are similar in the upper mantle; therefore, large differences in splitting between these phases can generally be attributed to anisotropy in the lowermost mantle. This assumption is generally valid if the difference in splitting due to deep mantle anisotropy is sufficiently large (e.g., Tesoniero et al., 2020), although it has been shown that small differences in SKS-SKKS splitting can be due to upper mantle structure (e.g., Lin et al., 2014).

Wookey et al. (2005) developed the S-ScS differential splitting technique, which has been widely used since then (e.g., Asplet et al., 2023; Creasy et al., 2017; Nowacki et al., 2010; Pisconti et al., 2023). This method exploits the fact that S and ScS waves have very similar raypaths in the upper mantle beneath the source and receiver. However, only ScS potentially experiences shear wave splitting due to deep mantle anisotropy and this contribution can be extracted by comparison to S splitting. The validity and potential pitfalls of this method have been thoroughly investigated using full-wave simulations (Nowacki & Wookey, 2016; Wolf et al., 2022a, 2022b). It has been demonstrated that the initial implementation of the S-ScS differential splitting technique, which does not explicitly account for the radial component phase shift due to the CMB reflection, can introduce apparent splitting under certain circumstances even when D″ anisotropy is not present (Wolf et al., 2022a). Specifically,

Table 1
Studies (First Column) That Have Suggested the Presence of Deep Mantle Seismic Anisotropy Based on Body Wave Analysis

Study	Region	Modeled flow directions
1. Differential SV-SH travel times (S, S_{diff}, ScS)		
Lay and Helmberger (1983)[iso]	Caribbean	No
Lay and Young (1991)	Alaska	No
Vinnik et al. (1995)	Central Pacific	No
Kendall and Silver (1996)	Caribbean	No
Matzel et al. (1996)	Alaska	No
Ding and Helmberger (1997)	Caribbean	No
Garnero and Lay (1997)	Alaska	No
Vinnik et al. (1998)	Central Pacific	No
Ritsema et al. (1998)	Central Pacific	No
Pulliam and Sen (1998)	Central Pacific	No
Russell et al. (1998)	Central Pacific	No
Kendall and Silver (1998)[iso]	Central Pacific	No
Russell et al. (1999)	Central Pacific	No
Wysession et al. (1999)	Alaska	No
Ritsema (2000)	Indian Ocean	No
Fouch et al. (2001)	Alaska	No
Thomas and Kendall (2002)	North Asia	No
Garnero, Moore, et al. (2004)[iso]	Atlantic Ocean	No
Rokosky et al. (2004)	Caribbean	No
Rokosky et al. (2006)	Caribbean	No
S. R. Ford et al. (2006)	South Pacific	No
Thomas et al. (2007)	Southeast Asia	No
Usui et al. (2008)	Antarctic Ocean	No
Yang et al. (2008)	North Asia	No
2. Polarities (S, SdS, PdP)		
Garnero, Maupin, et al. (2004)	Caribbean	No
Maupin et al. (2005)	Caribbean	No
Thomas et al. (2011)	North Asia; Caribbean	No
Pisconti et al. (2019)	Atlantic Ocean	Northeast
Pisconti et al. (2023)	Atlantic Ocean	East-Northeast
3. SKS-SKKS-S3KS-PKS differential splitting		
Wang and Wen (2004)	West Africa	No
Niu and Perez (2004)	Single paths across globe	No
Long (2009)	Eastern Pacific	No
He and Long (2011)	Western Pacific	No
Vanacore and Niu (2011)	Northwest Pacific Ocean	Upwelling
Lynner and Long (2012)	Central Africa	No
Lynner and Long (2014)	Africa; South Europe	No
Roy et al. (2014)	Southeast Asia	No
Long and Lynner (2015)	East Europe	No
H. A. Ford et al. (2015)	West Africa	Horizontal and upwelling

Table 1
Continued

Study	Region	Modeled flow directions
Creasy et al. (2017)	Indian Ocean; Antarctic Ocean	Inconclusive; North-northeast/South-southwest
Deng et al. (2017)	East Pacific Ocean	No
Wolf et al. (2019)	North Europe	Horizontal, upwelling
Grund and Ritter (2019)	Central, Northern Europe; North Asia	No
Reiss et al. (2019)[iso]	South Europe; Africa	Northwest/Southeast; Southwest, upwelling
Asplet et al. (2020)	Northeast Pacific Ocean	No
Lutz et al. (2020)	Western USA	~West
Creasy et al. (2021)	North Asia	North-Northeast/South-southwest
Wolf and Long (2022)	Northeast Pacific Ocean	South
Wolf et al. (2023a)	Northeast Pacific Ocean; Western USA	No
Asplet et al. (2023)	Northeast Pacific Ocean	Northwest or Southwest/up-downwelling
Wolf and Long (2023)	Southeast Asia	Southwest
4. S-ScS differential splitting		
Wookey et al. (2005)	Northwest Pacific	No
Wookey and Kendall (2008)	North Asia	South
Nowacki et al. (2010)	Western USA; Caribbean	No
H. A. Ford et al. (2015)	West Africa	Horizontal and upwelling
Creasy et al. (2017)	Indian Ocean; Antarctic Ocean	Inconclusive; North-northeast/South-southwest
Rao et al. (2017)	Indian Ocean	No
Pisconti et al. (2019)[iso]	Atlantic Ocean	Northeast
Wolf et al. (2019)	Northern Europe	Horizontal and upwelling
Creasy et al. (2021)	North Asia	North-Northeast/South-southwest
Wolf et al. (2022a)	East Asia	No
Pisconti et al. (2023)[iso]	Atlantic Ocean	East-Northeast
Asplet et al. (2023)	Northeast Pacific Ocean	Northwest or Southwest/up-downwelling
5. Regional anisotropic inversions		
Kawai and Geller (2010)	Central Pacific Ocean	No
Suzuki et al. (2021)	North Pacific Ocean; Alaska	No

Note. The table is primarily ordered by the method used to detect seismic anisotropy, and secondarily ordered by the year of publication. The second column indicates the region for which deep mantle anisotropy has been suggested, and the third column lists whether flow directions were modeled, and if so, which directions are considered to be most likely. If *iso* is appended to the study name in the first column, this indicates that the authors interpret at least some of their observations as likely indicative of the absence of D″ anisotropy. These interpretations are difficult to account for objectively in the context of our compiled database, but we still report them in this table.

measurements are accurate when the source-side anisotropy contribution is absent or small, or when ScS is initially (nearly) completely SH-polarized due to the source mechanism. However, artifacts may be introduced in other circumstances (Wolf et al., 2022a). Furthermore, full-wave (i.e., non-ray theoretical) effects have been shown to be important for heterogeneous anisotropy (e.g., Nowacki & Wookey, 2016; Wolf et al., 2022b).

Anisotropic inversions that focus on a specific region represent another approach to investigate D″ anisotropy (Kawai & Geller, 2010; Suzuki et al., 2021). Such studies have used full seismic waveforms around the S and ScS arrival times at teleseismic distances to invert for radial anisotropy. These studies, by construction, consider full-wave effects but are sometimes hard to compare to splitting studies due to the simplified assumption of radial anisotropy.

A relatively recent development is the implementation of S_{diff} splitting measurements that explicitly consider the initial source polarization of S_{diff} (e.g., Cottaar & Romanowicz, 2013; Wolf & Long, 2022) (in the following abbreviated as $S_{diff,pol}$ splitting measurements). These measurements are compatible with the results of previous
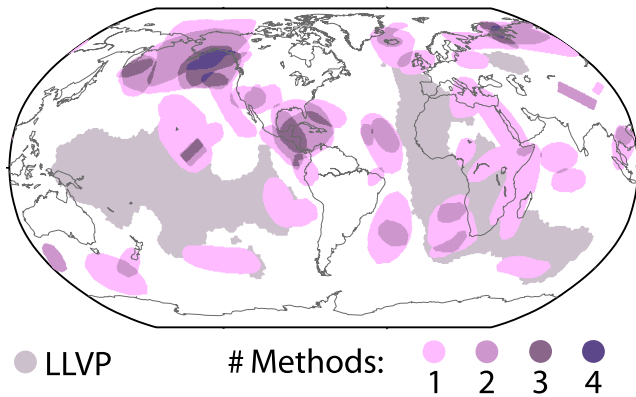
Figure 1. Locations for which the presence of deep mantle seismic anisotropy has been suggested in previous studies. The number of methods used to analyze deep mantle anisotropy in these regions is shown with violet shading (see legend), using the method categorization from Table 1. Low velocity features are shown in gray as determined by regions where at least 3 out of 5 tomography models assigned a particular point to a slow cluster at a depth of 2,700 km in the cluster analysis performed by Lekic et al. (2012).

studies that have shown that differential SV-SH times can be accumulated in an isotropic structure (e.g., Borgeaud et al., 2016; Komatitsch et al., 2010; Parisi et al., 2018) and have been tested in detail using global wavefield simulations (Wolf et al., 2023b).

This suite of body wave methods to observe D″ anisotropy is sensitive to different aspects of anisotropic geometry. For example, the regional anisotropic inversions for D″ anisotropy that have been conducted to date, by construction, resolve radial anisotropy. Splitting studies, often resolve more complex anisotropy with an azimuthal component; however, the sensitivity to different types of anisotropy depends on the raypath geometry. For example, SKS, SKKS, and ScS waves generally sample D″ obliquely, but SKS is often closer to vertical and ScS closer to the horizontal (Figure 2), although the details depend on the raypath configurations. Similarly, S_{diff} splitting results have often been interpreted in terms of radial anisotropy. However, using a single measurement, it is impossible to distinguish whether seismic anisotropy is sampled while S_{diff} travels horizontally along the CMB or obliquely through D″. Therefore, for a single S_{diff} measurement, it is hard to distinguish between radial anisotropy, sampled at the CMB and more complex seismic anisotropy sampled on the upgoing (or downgoing) leg through D″.

3. Compilation of D″ Anisotropy Locations

We compile and digitize the full set of lowermost mantle locations for which previous studies have suggested the presence of D″ anisotropy, as presented in the original publications. These locations are hand-digitized based mostly on the figures provided in the studies, but also based on information given in text and corresponding supplementary materials. We present a global map of these previously suggested deep mantle anisotropy locations in Figure 1 and different sub-data sets for different analysis methods in Figures 2a–2f. The reason for distinguishing between different splitting strategies is that each of them has distinct strengths and weaknesses, as described in Section 2. Despite these differences, we chose to incorporate all previous studies in our analysis. Users of the database can choose themselves which studies they consider relevant for their research purpose. The full list of studies, grouped using the method used to analyze deep mantle anisotropy, and further grouped by year of publication, is shown in Table 1. Overall, seismic anisotropy has been found for ∼26% of D″.

4. Statistical Analysis: Is There a Spatial Correlation Between Anisotropy Locations and LLVP Edges?

We conduct a statistical analysis on the global data set, with the specific goal of testing whether deep mantle seismic anisotropy is more likely to be found near the edges of LLVPs than elsewhere. For this analysis, we create a regular, equally spaced, spherical grid with 10,242 grid points, leading to a spacing of 2.5° between grid points (and thus using equal area bins). For each grid point, we check whether it marks a location at which D″ mantle anisotropy has been suggested previously or not. We then calculate the shortest distance of each grid point that indicates deep mantle anisotropy to the border of the nearest LLVPs in the deep mantle. We determine these borders by defining LLVP locations as regions where at least 3 out of 5 tomography models show low velocity structures at 2,700 km depth in the cluster analysis of Lekic et al. (2012). Finally, we calculate the average distance of all grid points marking deep mantle seismic anisotropy to the nearest edge of an LLVP. The precise LLVP edge locations are used in these calculations, as defined above, without interpolation to the grid. For comparison, we generate a set of 1,000 random distributions of deep mantle anisotropy by applying 1,000 uniform random spherical rotations of the actual anisotropy distribution (i.e., maintaining the relative orientation of regions). We then repeat our minimum distance calculations for each distribution. Finally, we compare our results using the actual distribution with the results using the distribution of average distances obtained through the random rotations. Unfortunately, reports of null detections of deep mantle anisotropy are rare in the literature and cannot be usefully incorporated into our analysis.

Our statistical analysis shows that the mean distance of D″ anisotropy locations to the nearest LLVP regions approximately agrees with the mean value obtained from the 1,000 random rotations (Figure 3a), suggesting that there is no global spatial correlation of D″ anisotropy with the edges of LLVPs. We also conducted separate
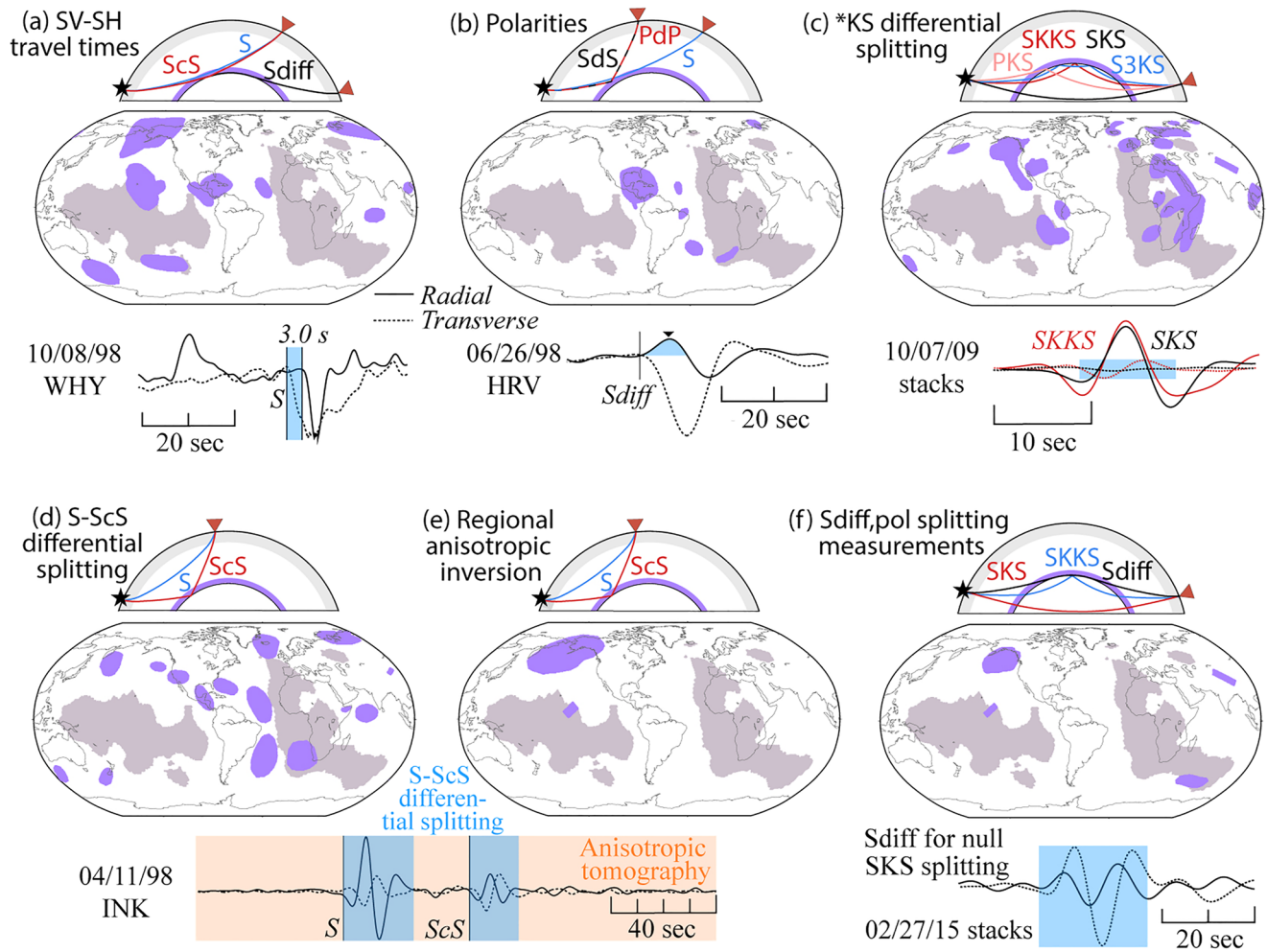
Figure 2. Summary of D″ anisotropy distribution, based on different measurement methods and ordered as in Table 1. (a) Top: Cross-section of seismic phases used to determine differential SV-SH travel times. The source is represented as a black star and stations as red triangles. Middle: Seismic anisotropy locations identified using differential SV-SH travel times. The plotting conventions are as in Figure 1. Bottom: Real data example after Garnero, Maupin, et al. (2004), showing a differential arrival time for the S seismic phase in radial and transverse component seismograms (blue shading). The waveforms were recorded at station WHY for an event that occurred on 8 October 1998. (b) Polarity studies; the real data example is after Garnero and Lay (2003) and shows an anomalous radial component S_{diff} polarity (blue shading). Otherwise, as in all other panels, plotting conventions are the same as in panel (a). (c) *KS differential splitting measurements; the real data example is after Wolf and Long (2022) and shows differential splitting of SKS and SKKS (blue shading). (d) S-ScS differential splitting; the real data example of S and ScS waveforms is after Wolf et al. (2019) (blue shading). (e) Regional anisotropic inversions; real data example of a seismogram around S and ScS arrivals (orange shading) is as in panel (d). (f) S_{diff} splitting measurements that explicitly consider the wave's initial polarization; the real data example is after Wolf and Long (2023), showing an example radial and transverse S_{diff} waveforms that exhibit splitting for a case in which SKS splitting is null (blue shading).

analyses for D″ anisotropy locations detected using three particularly commonly used methods, including SKS-SKKS differential splitting, S-ScS differential splitting and S_{diff} observations (differential travel times and/or $S_{diff,pol}$ splitting measurements). This consideration separately allows us to explicitly consider the global ray coverage for each method (Section 5), as different epicentral distances are used for each. The results show that D″ anisotropy is, on average, slightly farther away from the LLVP edges than for a set of 1,000 random rotations of D″ anisotropy for S_{diff} and S-ScS. For SKS-SKKS differential splitting, D″ anisotropy is slightly closer to an LLVP edge than expected for the random distribution. However, these differences are slight and we do not view them as statistically significant.

5. Discussion

While our straightforward statistical analysis is informative, it does not consider several potential factors influencing the distribution of previously detected deep mantle anisotropy locations. For example, it is immedi-
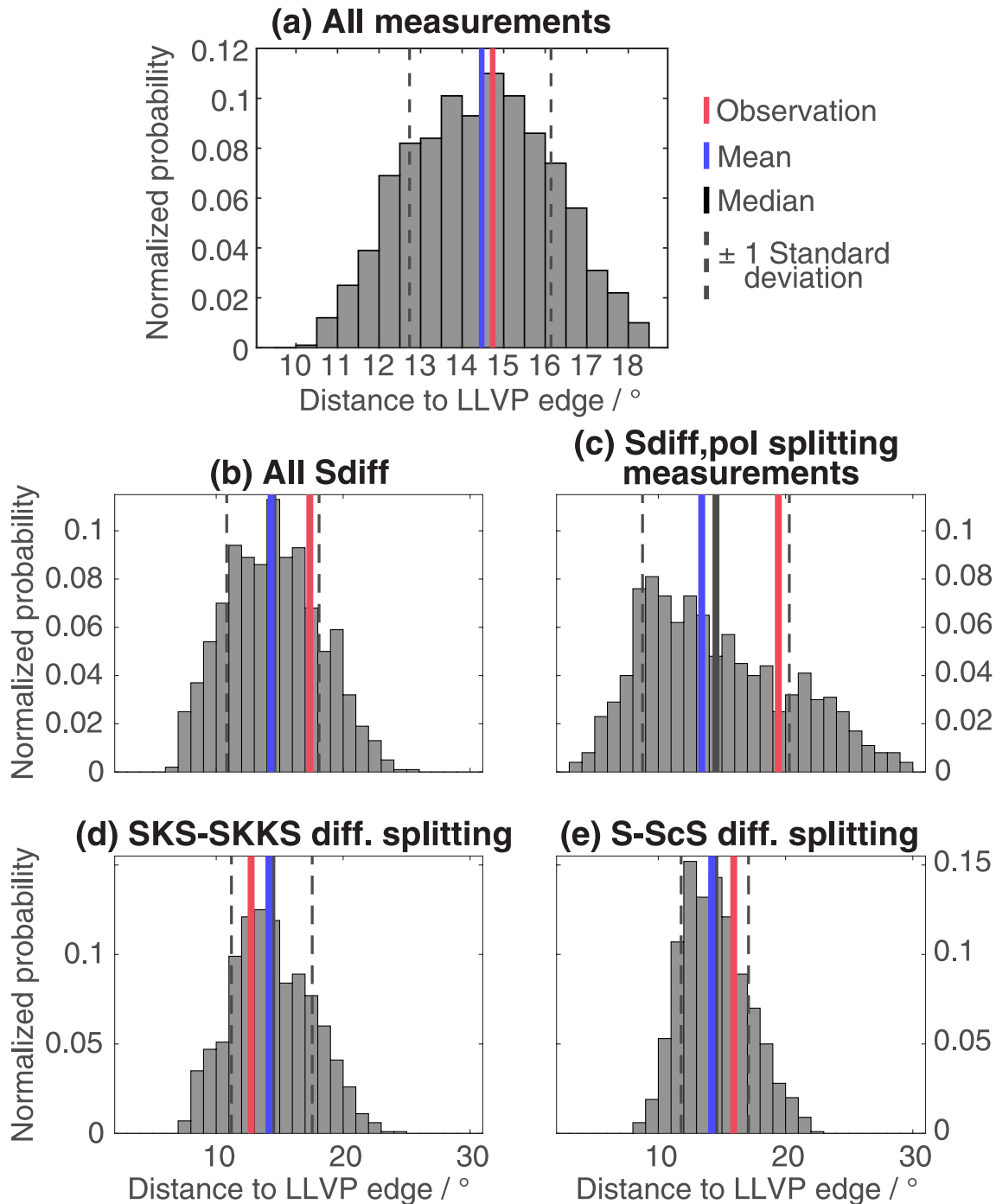
Figure 3. Statistical assessment of the spatial correlation between large-low velocity province edges and seismic anisotropy. (a) Histogram (gray) for 1,000 random spherical rotations of all deep mantle anisotropy locations (Section 4). The mean of the distribution is shown by a solid blue vertical line and the median as a black line (see legend). (Mean and median are identical for this distribution). One standard deviation of the random distribution is shown on both sides as vertical dashed black lines. The result of the actual deep mantle anisotropy distribution (Figure 1) is shown as a vertical solid red line. (b) Same as panel (a), for all studies that use S_{diff} to measure deep mantle anisotropy. (c) Same as panel (a), for S_{diff} splitting measurements that explicitly consider the wave's initial polarization. (The deviation from a normal distribution is due to the small number of measurements made with this method, as shown in Figure 2f.) (d) Same as panel (a), for SKS-SKKS differential splitting. (e) Same as panel (a), for S-ScS differential splitting.

ately apparent in Figure 1 that fewer D″ anisotropy locations have been identified in the southern than in the northern hemisphere. This observation is unlikely to be linked to mantle dynamics but is rather caused by the unequal global ray coverage. To interrogate whether and how ray coverage influences the results of our statistical

correlation, we consider the ray coverage in the D″ layer for the different data subsets shown in Figure 3. Expanding upon previous work (e.g., Creasy et al., 2019), we report ray coverage individually for each method that can be used to diagnose D″ anisotropy, including S_{diff} splitting, using realistic source-receiver configurations. Because our aim is to illustrate which regions are well-sampled by commonly used splitting methods and where seismic anisotropy has and has not (yet) been detected, we do not include PdP and SdS polarity measurements here. Such measurements are usually used as an additional constraint along with complementary splitting data (e.g., Pisconti et al., 2019, 2023) rather than being interpreted as uniquely indicative of deep mantle anisotropy. We estimate this ray coverage by considering all events with moment magnitudes 6 or larger (according to the International Seismological Center Bulletin, International Seismological Centre (2023)) that occurred between January 1990 and March 2023, and the station distribution covered by most common data request clients (see Acknowledgments). We use ObsPy (Beyreuther et al., 2010) to calculate the lowermost mantle ray coverage of S_{diff} (epicentral distance 103°–125°; Figure 4a), SKS-SKKS (epicentral distance 108°–122°; Figure 4b), and S-ScS (epicentral distance 60°–85°; Figure 4c) at the epicentral distances used in splitting studies. We combine these results in Figure 4d for a map of global ray coverage using any of these methods. For each splitting method, we assign every grid point a number between 1 and 0, based on the number of rays that sample it, normalized to the maximum number of rays globally for any grid point (Figure 4). Figure 4 shows that D″ seismic anisotropy has been suggested in many well-sampled regions, but not in all of them.

This exercise demonstrates that it is essential to consider ray coverage when assessing the spatial distribution of deep mantle seismic anisotropy. However, ray coverage is difficult to quantitatively account for a statistical analysis such as that discussed in Section 4. One approach to understanding how well-sampled LLVP edges are compared to the global average is to compare the mean and median ray coverage of bins that mark LLVP edges with the global mean and median ray coverage. For the methods investigated in Figure 4, both the mean and medium ray coverage tends to be ~20% lower at the LLVP edges than for the global average. This discrepancy may influence the results of our statistical analysis, which implicitly assumes equal ray coverage throughout the deep mantle. The raypath sampling maps (Figure 4) can be used to determine new target regions with dense raypath coverage for which seismic anisotropy has not yet been analyzed in past studies.

Another factor potentially influencing our analysis is the difficulty of conclusively identifying the absence of anisotropy in D″. While null splitting measurements for deep mantle anisotropy are regularly reported for specific raypaths (e.g., Asplet et al., 2020; H. A. Ford et al., 2015; Garnero, Maupin, et al., 2004; Reiss et al., 2019), they are only sometimes interpreted as being indicative of an isotropic D″ (Table 1). The reason is that a null measurement along a single raypath cannot, by itself, rule out the presence of seismic anisotropy, and confirmation of the absence of seismic anisotropy in the region under study requires raypath sampling from multiple directions. Previous studies have handled this issue in different ways: Some explicitly invoke isotropy as a likely explanation if no splitting is observed from a single direction (e.g., Kendall & Silver, 1998; Pisconti et al., 2019; Reiss et al., 2019), while other studies are more cautious (e.g., H. A. Ford et al., 2015; Wolf & Long, 2023) in their interpretation. Some studies that measure null splitting for certain sampling directions explicitly consider the possibility that they have sampled a null direction of the anisotropy (Asplet et al., 2023; H. A. Ford et al., 2015). While investigators may be aware of this ambiguity, whether they find their observations sufficiently indicative of isotropy is a matter of interpretation. Therefore, it is very challenging to consider null measurements of D″ anisotropy in a global analysis.

Apart from uneven ray coverage, there are other potential factors that may influence the results of our statistical analysis. For example, our results are potentially influenced by the fact that after it had been suggested that D″ seismic anisotropy may be stronger along LLVP edges based on regional studies (e.g., Cottaar & Romanowicz, 2013; Wang & Wen, 2004), subsequent studies may have tended to preferentially search for D″ anisotropy at these edges. Again, this factor is difficult to quantify. Investigations of correlations that include estimates of anisotropy strength, rather than a binary finding of anisotropy detected/not detected, would be highly desirable, but are currently extremely challenging. Anisotropy strengths determined using different methods are not necessarily comparable, as raypaths are different, methods are sensitive to different types of anisotropy (e.g., radial or azimuthal anisotropy; see Section 2), and the apparent anisotropic strengths depend on the sampling direction. Additional uncertainty is added by the subjective definition of exactly where the LLVP edge is located. Estimates of LLVP edge locations can vary between different tomography models, in some places by as much as 1,000 km (e.g., Garnero et al., 2016; Lekic et al., 2012).
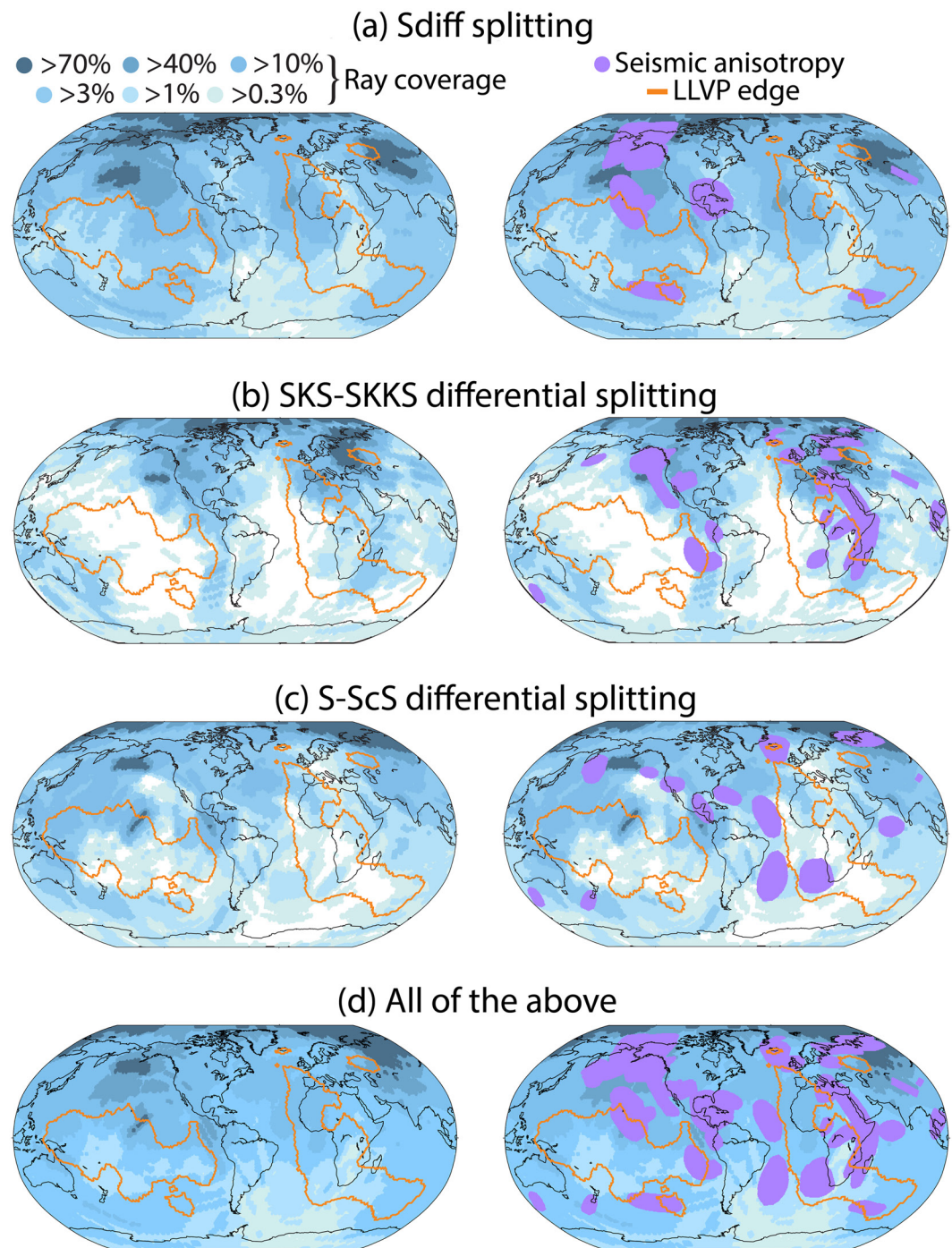
Figure 4. Global raypath coverage for (a) S_{diff}, (b) SKS-SKKS differential splitting, (c) S-ScS differential splitting measurements, and (d) all these methods together, calculated for all events with moment magnitudes greater than 6 between January 1990 and March 2023. Ray coverage is reported relative to the maximum bin (100%, see legend). Large-low velocity province edges are indicated by orange lines. The right column additionally shows locations for which the presence of seismic anisotropy has been previously suggested (violet color), hinting at which regions with good coverage the different techniques can be applied to in future studies.

One simple question that we can answer with our compiled database is whether previously suggested locations of deep mantle anisotropy are primarily located within or outside of LLVPs. Overall, 33% of the sampled area of D′′ outside LLVPs has been found to be anisotropic, while this value is only 21% inside the LLVPs. The significance

of this observation, however, is influenced by the same caveats as the potential correlation with LLVP edges. In particular, ray coverage within LLVPs tends to be poorer than outside them (Figure 4); therefore, it is less likely that seismic anisotropy is detected within LLVPs than elsewhere.

Because of the caveats discussed above, whether D′′ anisotropy preferentially occurs near LLVP edges on a global scale remains inconclusive. With the increasing availability of D′′ seismic anisotropy studies, however, this question can be more confidently pursued in future work. One way to do this is to apply a uniform methodology to investigate deep mantle anisotropy globally, exploiting all available seismic data (Figure 4). Seismic anisotropy can also be predicted through geodynamic modeling calculations (Chandler et al., 2021; Cottaar et al., 2014; Walker et al., 2011). Therefore, our understanding of the global distribution of seismic anisotropy in the D′′ layer and its relation with the lowermost mantle structures and dynamics can also be improved by comparing seismically determined anisotropy models with results of geodynamic modeling experiments.

6. Conclusion

We create and make available a global digital database of locations at which seismic anisotropy in the D′′ layer has been detected using a variety of body wave phases. We encourage researchers to reach out to the corresponding author to add new data sets and results to the database and plan to regularly update it as new studies are published. Using this database at the time of writing, we show that on a global scale, deep mantle seismic anisotropy is not more likely to be found at the edges of the LLVPs than a random distribution would suggest. One factor influencing our statistical assessment is ray coverage, which tends to be poorer than the global average at LLVP edges, although this factor is difficult to explicitly account for our analysis.

Data Availability Statement

The compiled database of deep mantle anisotropy locations is available at a data repository (Wolf et al., 2023c) and https://github.com/wolfjonathan/Deep_Mantle_Anisotropy_Database.

References

Asplet, J., Wookey, J., & Kendall, M. (2020). A potential post-perovskite province in D′′ beneath the eastern Pacific: Evidence from new analysis of discrepant SKS–SKKS shear-wave splitting. *Geophysical Journal International*, *221*(3), 2075–2090. https://doi.org/10.1093/gji/ggaa114

Asplet, J., Wookey, J., & Kendall, M. (2023). Inversion of shear wave waveforms reveal deformation in the lowermost mantle. *Geophysical Journal International*, *232*(1), 97–114. https://doi.org/10.1093/gji/ggac328

Barruol, G., & Kern, H. (1996). Seismic anisotropy and shear-wave splitting in lower-crustal and upper-mantle rocks from the Ivrea zone: Experimental and calculated data. *Physics of the Earth and Planetary Interiors*, *95*(3–4), 175–194. https://doi.org/10.1016/0031-9201(95)03124-3

Bercovici, D., & Karato, S. (2003). Whole-mantle convection and the transition-zone water filter. *Nature*, *425*(6953), 39–44. https://doi.org/10.1038/nature01918

Beyreuther, M., Barsch, R., Krischer, L., Megies, T., Behr, Y., & Wassermann, J. (2010). ObsPy: A python toolbox for seismology. *Seismological Research Letters*, *81*(3), 530–533. https://doi.org/10.1111/10.1785/gssrl.81.3.530

Borgeaud, A. F., Konishi, K., Kawai, K., & Geller, R. J. (2016). Finite frequency effects on apparent S-wave splitting in the D′′ layer: Comparison between ray theory and full-wave synthetics. *Geophysical Journal International*, *207*(1), 12–28. https://doi.org/10.1093/gji/ggw254

Chandler, B. C., Chen, L.-W., Li, M., Romanowicz, B., & Wenk, H.-R. (2021). Seismic anisotropy, dominant slip systems and phase transitions in the lowermost mantle. *Geophysical Journal International*, *227*(3), 1665–1681. https://doi.org/10.1093/gji/ggab278

Chang, S.-J., Ferreira, A. M. G., Ritsema, J., van Heijst, H. J., & Woodhouse, J. H. (2015). Joint inversion for global isotropic and radially anisotropic mantle structure including crustal thickness perturbations. *Journal of Geophysical Research: Solid Earth*, *120*(6), 4278–4300. https://doi.org/10.1002/2014JB011824

Cottaar, S., Li, M., McNamara, A. K., Romanowicz, B., & Wenk, H.-R. (2014). Synthetic seismic anisotropy models within a slab impinging on the core–mantle boundary. *Geophysical Journal International*, *199*(1), 164–177. https://doi.org/10.1093/gji/ggu244

Cottaar, S., & Romanowicz, B. (2013). Observations of changing anisotropy across the southern margin of the African LLSVP. *Geophysical Journal International*, *195*(2), 1184–1195. https://doi.org/10.1093/gji/ggt285

Creasy, N., Long, M. D., & Ford, H. A. (2017). Deformation in the lowermost mantle beneath Australia from observations and models of seismic anisotropy. *Journal of Geophysical Research: Solid Earth*, *122*(7), 5243–5267. https://doi.org/10.1002/2016JB013901

Creasy, N., Pisconti, A., Long, M. D., & Thomas, C. (2021). Modeling of seismic anisotropy observations reveals plausible lowermost mantle flow directions beneath Siberia. *Geochemistry, Geophysics, Geosystems*, *22*(10), e2021GC009924. https://doi.org/10.1029/2021GC009924

Creasy, N., Pisconti, A., Long, M. D., Thomas, C., & Wookey, J. (2019). Constraining lowermost mantle anisotropy with body waves: A synthetic modelling study. *Geophysical Journal International*, *217*(2), 766–783. https://doi.org/10.1093/gji/ggz049

Deng, J., Long, M. D., Creasy, N., Wagner, L., Beck, S., Zandt, G., et al. (2017). Lowermost mantle anisotropy near the eastern edge of the Pacific LLSVP: Constraints from SKS-SKKS splitting intensity measurements. *Geophysical Journal International*, *210*(2), 774–786. https://doi.org/10.1093/gji/ggx190

Ding, X., & Helmberger, D. V. (1997). Modelling D′′ structure beneath Central America with broadband seismic data. *Physics of the Earth and Planetary Interiors*, *101*(3–4), 245–270. https://doi.org/10.1016/S0031-9201(97)00001-0

Erdman, M. E., Hacker, B. R., Zandt, G., & Seward, G. (2013). Seismic anisotropy of the crust: Electron-backscatter diffraction measurements from the basin and range. *Geophysical Journal International*, *195*(2), 1211–1229. https://doi.org/10.1093/gji/ggt287

Ford, H. A., Long, M. D., He, X., & Lynner, C. (2015). Lowermost mantle flow at the eastern edge of the African large low shear velocity province. *Earth and Planetary Science Letters*, *420*, 12–22. https://doi.org/10.1016/j.epsl.2015.03.029

Ford, S. R., Garnero, E. J., & McNamara, A. K. (2006). A strong lateral shear velocity gradient and anisotropy heterogeneity in the lowermost mantle beneath the southern pacific. *Journal of Geophysical Research*, *111*(B3), B03306. https://doi.org/10.1029/2004JB003574

Fouch, M. J., Fischer, K. M., & Wysession, M. E. (2001). Lowermost mantle anisotropy beneath the Pacific: Imaging the source of the Hawaiian plume. *Earth and Planetary Science Letters*, *190*(3–4), 167–180. https://doi.org/10.1016/S0012-821X(01)00380-6

Garnero, E. J., & Lay, T. (1997). Lateral variations in lowermost mantle shear wave anisotropy beneath the north Pacific and Alaska. *Journal of Geophysical Research*, *102*(B4), 8121–8135. https://doi.org/10.1029/96JB03830

Garnero, E. J., & Lay, T. (2003). D′′ shear velocity heterogeneity, anisotropy and discontinuity structure beneath the Caribbean and Central America. *Physics of the Earth and Planetary Interiors*, *140*(1–3), 219–242. https://doi.org/10.1016/j.pepi.2003.07.014

Garnero, E. J., Maupin, V., Lay, T., & Fouch, M. J. (2004). Variable azimuthal anisotropy in Earth's lowermost mantle. *Science*, *306*(5694), 259–261. https://doi.org/10.1126/science.1103411

Garnero, E. J., McNamara, A., & Shim, S.-H. (2016). Continent-sized anomalous zones with low seismic velocity at the base of Earth's mantle. *Nature Geoscience*, *9*(7), 481–489. https://doi.org/10.1038/ngeo2733

Garnero, E. J., Moore, M. M., Lay, T., & Fouch, M. J. (2004). Isotropy or weak vertical transverse isotropy in D′′ beneath the Atlantic Ocean. *Journal of Geophysical Research*, *109*(B8), 1–10. https://doi.org/10.1029/2004JB003004

Grund, M., & Ritter, J. R. (2019). Widespread seismic anisotropy in Earth's lowermost mantle beneath the Atlantic and Siberia. *Geology*, *47*(2), 123–126. https://doi.org/10.1130/G45514.1

He, X., & Long, M. D. (2011). Lowermost mantle anisotropy beneath the northwestern Pacific: Evidence from PcS, ScS, SKS, and SKKS phases. *Geochemistry, Geophysics, Geosystems*, *12*, Q12012. https://doi.org/10.1029/2011GC003779

Hernlund, J., Thomas, C., & Tackley, P. (2005). A doubling of the post-perovskite phase boundary and structure of the Earth's lowermost mantle. *Nature*, *434*(7035), 882–886. https://doi.org/10.1016/10.1038/nature03472

International Seismological Centre. (2023). On-line bulletin. https://doi.org/10.31905/D808B830

Kawai, K., & Geller, R. J. (2010). The vertical flow in the lowermost mantle beneath the Pacific from inversion of seismic waveforms for anisotropic structure. *Earth and Planetary Science Letters*, *297*(1), 190–198. https://doi.org/10.1016/j.epsl.2010.05.037

Kendall, J.-M., & Silver, P. (1996). Constraints from seismic anisotropy on the nature of the lower mantle. *Nature*, *381*(6581), 409–412. https://doi.org/10.1038/381409a0

Kendall, J.-M., & Silver, P. (1998). Investigating causes of D′′ anisotropy. In *The core-mantle boundary region*, Geodynamic Series (Vol. 28, pp. 97–118).

Komatitsch, D., Vinnik, L. P., & Chevrot, S. (2010). SHdiff-SVdiff splitting in an isotropic Earth. *Journal of Geophysical Research*, *115*(B7), B07312. https://doi.org/10.1029/2009JB006795

Lay, T., & Helmberger, D. V. (1983). The shear-wave velocity gradient at the base of the mantle. *Journal of Geophysical Research*, *88*(B10), 8160–8170. https://doi.org/10.1029/JB088iB10p08160

Lay, T., Williams, Q., Garnero, E. J., Kellogg, L., & Wysession, M. E. (1998). Seismic wave anisotropy in the D′′ region and its implications. In *The core-mantle boundary region* (pp. 299–318). American Geophysical Union (AGU). https://doi.org/10.1029/GD028p0299

Lay, T., & Young, C. J. (1991). Analysis of seismic SV waves in the core's penumbra. *Geophysical Research Letters*, *18*(8), 1373–1376. https://doi.org/10.1029/91GL01691

Lekic, V., Cottaar, S., Dziewonski, A., & Romanowicz, B. (2012). Cluster analysis of global lower mantle tomography: A new class of structure and implications for chemical heterogeneity. *Earth and Planetary Science Letters*, *357–358*, 68–77. https://doi.org/10.1016/j.epsl.2012.09.014

Li, M., & Zhong, S. (2017). The source location of mantle plumes from 3D spherical models of mantle convection. *Earth and Planetary Science Letters*, *478*, 47–57. https://doi.org/10.1016/j.epsl.2017.08.033

Lin, Y.-P., Zhao, L., & Hung, S.-H. (2014). Full-wave effects on shear wave splitting. *Geophysical Research Letters*, *41*(3), 799–804. https://doi.org/10.1002/2013GL058742

Long, M. D. (2009). Complex anisotropy in D′′ beneath the eastern Pacific from SKS–SKKS splitting discrepancies. *Earth and Planetary Science Letters*, *283*(1–4), 181–189. https://doi.org/10.1016/j.epsl.2009.04.019

Long, M. D., & Becker, T. (2010). Mantle dynamics and seismic anisotropy. *Earth and Planetary Science Letters*, *297*(3–4), 341–354. https://doi.org/10.1016/j.epsl.2010.06.036

Long, M. D., & Lynner, C. (2015). Seismic anisotropy in the lowermost mantle near the Perm Anomaly. *Geophysical Research Letters*, *42*(17), 7073–7080. https://doi.org/10.1002/2015GL065506

Long, M. D., & Silver, P. G. (2009). Shear wave splitting and mantle anisotropy: Measurements, interpretations, and new directions. *Surveys in Geophysics*, *30*(4–5), 407–461. https://doi.org/10.1007/s10712-009-9075-1

Lutz, K., Long, M., Creasy, N., & Deng, J. (2020). Seismic anisotropy in the lowermost mantle beneath North America from SKS-SKKS splitting intensity discrepancies. *Physics of the Earth and Planetary Interiors*, *305*, 106504. https://doi.org/10.1016/j.pepi.2020.106504

Lynner, C., & Long, M. (2012). Evaluating contributions to SK(K)S splitting from lower mantle anisotropy: A case study from station DBIC, Cote d'Ivoire. *Bulletin of the Seismological Society of America*, *102*(3), 1030–1040. https://doi.org/10.1785/0120110255

Lynner, C., & Long, M. D. (2014). Lowermost mantle anisotropy and deformation along the boundary of the African LLSVP. *Geophysical Research Letters*, *41*(10), 3447–3454. https://doi.org/10.1002/2014GL059875

Matzel, E., Sen, M. K., & Grand, S. P. (1996). Evidence for anisotropy in the deep mantle beneath Alaska. *Geophysical Research Letters*, *23*(18), 2417–2420. https://doi.org/10.1029/96GL02186

Maupin, V., Garnero, E. J., Lay, T., & Fouch, M. J. (2005). Azimuthal anisotropy in the D′′ layer beneath the Caribbean. *Journal of Geophysical Research*, *110*(B8), B08301. https://doi.org/10.1029/2004JB003506

McNamara, A. K., Garnero, E. J., & Rost, S. (2010). Tracking deep mantle reservoirs with ultra-low velocity zones. *Earth and Planetary Science Letters*, *299*(1–2), 1–9. https://doi.org/10.1016/j.epsl.2010.07.042

McNamara, A. K., van Keken, P., & Karato, S.-I. (2002). Development of anisotropic structure in the Earth's lower mantle by solid-state convection. *Nature*, *416*(6878), 310–314. https://doi.org/10.1038/416310a

Niu, F., & Perez, A. M. (2004). Seismic anisotropy in the lower mantle: A comparison of waveform splitting of SKS and SKKS. *Geophysical Research Letters*, *31*(24), L24612. https://doi.org/10.1029/2004GL021196

Nowacki, A., & Wookey, J. (2016). The limits of ray theory when measuring shear wave splitting in the lowermost mantle with ScS waves. *Geophysical Journal International*, *207*(3), 1573–1583. https://doi.org/10.1093/gji/ggw358

Nowacki, A., Wookey, J., & Kendall, J.-M. (2010). Deformation of the lowermost mantle from seismic anisotropy. *Nature*, *467*(7319), 1091–1094. https://doi.org/10.1038/nature09507

Panning, M., & Romanowicz, B. (2006). A three-dimensional radially anisotropic model of shear velocity in the whole mantle. *Geophysical Journal International*, *167*(1), 361–379. https://doi.org/10.1111/j.1365-246X.2006.03100.x

Parisi, L., Ferreira, A. M. G., & Ritsema, J. (2018). Apparent splitting of S waves propagating through an isotropic lowermost mantle. *Journal of Geophysical Research: Solid Earth*, *123*(5), 3909–3922. https://doi.org/10.1002/2017JB014394

Pisconti, A., Creasy, N., Wookey, J., Long, M. D., & Thomas, C. (2023). Mineralogy, fabric and deformation domains in D″ across the southwestern border of the African LLSVP. *Geophysical Journal International*, *232*(1), 705–724. https://doi.org/10.1093/gji/ggac359

Pisconti, A., Thomas, C., & Wookey, J. (2019). Discriminating between causes of D″ anisotropy using reflections and splitting measurements for a single path. *Journal of Geophysical Research: Solid Earth*, *124*(5), 4811–4830. https://doi.org/10.1029/2018JB016993

Pulliam, J., & Sen, M. K. (1998). Seismic anisotropy in the core-mantle transition zone. *Geophysical Journal International*, *135*(1), 113–128. https://doi.org/10.1046/j.1365-246X.1998.00612.x

Rao, P. B., Kumar, M., & Singh, A. (2017). Anisotropy in the lowermost mantle beneath the Indian Ocean Geoid Low from ScS splitting measurements. *Geochemistry, Geophysics, Geosystems*, *18*, 13385–13393. https://doi.org/10.1002/2016GC006604

Reiss, M. C., Long, M. D., & Creasy, N. (2019). Lowermost mantle anisotropy beneath africa from differential SKS-SKKS shear-wave splitting. *Journal of Geophysical Research: Solid Earth*, *124*(8), 8540–8564. https://doi.org/10.1029/2018JB017160

Ritsema, J. (2000). Evidence for shear velocity anisotropy in the lowermost mantle beneath the Indian Ocean. *Geophysical Research Letters*, *27*(7), 1041–1044. https://doi.org/10.1029/1999GL011037

Ritsema, J., Lay, T., Garnero, E. J., & Benz, H. (1998). Seismic anisotropy in the lowermost mantle beneath the Pacific. *Geophysical Research Letters*, *25*(8), 1229–1232. https://doi.org/10.1029/98GL00913

Rokosky, J. M., Lay, T., & Garnero, E. J. (2006). Small-scale lateral variations in azimuthally anisotropic D″ structure beneath the Cocos Plate. *Earth and Planetary Science Letters*, *248*(1–2), 411–425. https://doi.org/10.1016/j.epsl.2006.06.005

Rokosky, J. M., Lay, T., Garnero, E. J., & Russell, S. A. (2004). High-resolution investigation of shear wave anisotropy in D″ beneath the Cocos Plate. *Geophysical Research Letters*, *31*(7), L07605. https://doi.org/10.1029/2003GL018902

Roy, S. K., Kumar, M. R., & Srinagesh, D. (2014). Upper and lower mantle anisotropy inferred from comprehensive SKS and SKKS splitting measurements from India. *Earth and Planetary Science Letters*, *392*, 192–206. https://doi.org/10.1016/j.epsl.2014.02.012

Russell, S. A., Lay, T., & Garnero, E. J. (1998). Seismic evidence for small-scale dynamics in the lowermost mantle at the root of the Hawaiian hotspot. *Nature*, *396*(6708), 255–258. https://doi.org/10.1038/24364

Russell, S. A., Lay, T., & Garnero, E. J. (1999). Small-scale lateral shear velocity and anisotropy heterogeneity near the core-mantle boundary beneath the central Pacific imaged using broadband ScS waves. *Journal of Geophysical Research*, *104*(B6), 13183–13199. https://doi.org/10.1029/1999JB900114

Savage, M. K. (1999). Seismic anisotropy and mantle deformation: What have we learned from shear wave splitting? *Reviews of Geophysics*, *37*(1), 65–106. https://doi.org/10.1016/10.1029/98RG02075

Silver, P. G. (1996). Seismic anisotropy beneath the continents: Probing the depths of geology. *Annual Review of Earth and Planetary Sciences*, *24*(1), 385–432. https://doi.org/10.1146/annurev.earth.24.1.385

Steinberger, B., & Torsvik, T. H. (2012). A geodynamic model of plumes from the margins of large low shear velocity provinces. *Geochemistry, Geophysics, Geosystems*, *13*(1), Q01W09. https://doi.org/10.1029/2011GC003808

Suzuki, Y., Kawai, K., & Geller, R. J. (2021). Imaging paleoslabs and inferring the Clapeyron slope in D″ beneath the northern Pacific based on high-resolution inversion of seismic waveforms for 3-D transversely isotropic structure. *Physics of the Earth and Planetary Interiors*, *321*, 106751. https://doi.org/10.1016/j.pepi.2021.106751

Tackley, P. J. (2000). Mantle convection and plate tectonics: Toward an integrated physical and chemical theory. *Science*, *288*(5473), 2002–2007. https://doi.org/10.1126/science.288.5473.2002

Tesoniero, A., Leng, K., Long, M. D., & Nissen-Meyer, T. (2020). Full wave sensitivity of SK(K)S phases to arbitrary anisotropy in the upper and lower mantle. *Geophysical Journal International*, *222*(1), 412–435. https://doi.org/10.1093/gji/ggaa171

Thomas, C., & Kendall, J.-M. (2002). The lowermost mantle beneath northern Asia—II. Evidence for lower-mantle anisotropy. *Geophysical Journal International*, *151*(1), 296–308. https://doi.org/10.1046/j.1365-246X.2002.01760.x

Thomas, C., Wookey, J., Brodholt, J., & Fieseler, T. (2011). Anisotropy as cause for polarity reversals of D′′ reflections. *Earth and Planetary Science Letters*, *307*(3–4), 369–376. https://doi.org/10.1016/j.epsl.2011.05.011

Thomas, C., Wookey, J., & Simpson, M. (2007). D″ anisotropy beneath southeast Asia. *Geophysical Research Letters*, *34*(4), L04301. https://doi.org/10.1029/2006GL028965

Usui, Y., Hiramatsu, Y., Furumoto, M., & Kanao, M. (2008). Evidence of seismic anisotropy and a lower temperature condition in the D″ layer beneath Pacific Antarctic Ridge in the Antarctic Ocean. *Physics of the Earth and Planetary Interiors*, *167*(3–4), 205–216. https://doi.org/10.1016/j.pepi.2008.04.006

Vanacore, E., & Niu, F. (2011). Characterization of the D″ beneath the Galapagos Islands using SKKS and SKS waveforms. *Earthquake Science*, *24*(1), 87–99. https://doi.org/10.1007/s11589-011-0772-8

Vinnik, L., Breger, L., & Romanowicz, B. (1998). Anisotropic structures at the base of the Earth's mantle. *Nature*, *393*(6685), 564–567. https://doi.org/10.1038/31208

Vinnik, L., Romanowicz, B., Le Stunff, Y., & Makeyeva, L. (1995). Seismic anisotropy in the D′′ layer. *Geophysical Research Letters*, *22*(13), 1657–1660. https://doi.org/10.1029/95GL01327

von Laven, K. (2019a). *Grid sphere*. MATLAB Central. Retrieved from https://www.mathworks.com/matlabcentral/fileexchange/28842-grid-sphere

von Laven, K. (2019b). *Nearest neighbor*. MATLAB Central. Retrieved from https://www.mathworks.com/matlabcentral/fileexchange/28844-find-nearest-neighbors-on-sphere

Walker, A. M., Forte, A. M., Wookey, J., Nowacki, A., & Kendall, J.-M. (2011). Elastic anisotropy of D″ predicted from global models of mantle flow. *Geochemistry, Geophysics, Geosystems*, *12*(10), Q10006. https://doi.org/10.1029/2011GC003732

Wang, Y., & Wen, L. (2004). Mapping the geometry and geographic distribution of a very low velocity province at the base of the Earth's mantle. *Journal of Geophysical Research*, *109*(B10), B10305. https://doi.org/10.1029/2003JB002674

Wenk, H.-R., & Romanowicz, B. (2017). Anisotropy in the deep Earth. *Physics of the Earth and Planetary Interiors*, *269*, 58–90. https://doi.org/10.1016/j.pepi.2017.05.005

Wessel, P., & Smith, W. H. F. (1998). New, improved version of generic mapping tools released. *Eos, Transactions American Geophysical Union*, *79*(47), 579. https://doi.org/10.1029/98EO00426

Wolf, J., Creasy, N., Pisconti, A., Long, M. D., & Thomas, C. (2019). An investigation of seismic anisotropy in the lowermost mantle beneath Iceland. *Geophysical Journal International*, *219*(Supplement_1), S152–S166. https://doi.org/10.1093/gji/ggz312

Wolf, J., & Evans, D. A. D. (2022). Reconciling supercontinent cycle models with ancient subduction zones. *Earth and Planetary Science Letters*, *578*, 117293. https://doi.org/10.1016/j.epsl.2021.117293

Wolf, J., Frost, D. A., Long, M. D., Garnero, E., Aderoju, A. O., Creasy, N., & Bozdağ, E. (2023a). Observations of mantle seismic anisotropy using array techniques: Shear-wave splitting of Beamformed SmKS phases. *Journal of Geophysical Research: Solid Earth*, *128*(1), e2022JB025556. https://doi.org/10.1029/2022JB025556

Wolf, J., & Long, M. D. (2022). Slab-driven flow at the base of the mantle beneath the northeastern Pacific Ocean. *Earth and Planetary Science Letters*, *594*, 117758. https://doi.org/10.1016/j.epsl.2022.117758

Wolf, J., & Long, M. D. (2023). *Slab-driven transport of ultra-low velocity material in the deep mantle*. EGU General Assembly 2023. https://doi.org/10.5194/egusphere-egu23-3947

Wolf, J., Long, M. D., Creasy, N., & Garnero, E. (2023b). On the measurement of Sdiff splitting caused by lowermost mantle anisotropy. *Geophysical Journal International*, *233*(2), 900–921. https://doi.org/10.1093/gji/ggac490

Wolf, J., Long, M. D., Leng, K., & Nissen-Meyer, T. (2022a). Constraining deep mantle anisotropy with shear wave splitting measurements: Challenges and new measurement strategies. *Geophysical Journal International*, *230*(1), 507–527. https://doi.org/10.1093/gji/ggac055

Wolf, J., Long, M. D., Leng, K., & Nissen-Meyer, T. (2022b). Sensitivity of SK(K)S and ScS phases to heterogeneous anisotropy in the lowermost mantle from global wavefield simulations. *Geophysical Journal International*, *228*(1), 366–386. https://doi.org/10.1093/gji/ggab347

Wolf, J., Long, M. D., Li, M., & Garnero, E. (2023c). Global compilation of deep mantle anisotropy observations and possible correlation with low velocity provinces - Dataset [Dataset]. Harvard Dataverse. https://doi.org/10.7910/DVN/EMJLDN

Wookey, J., & Kendall, J.-M. (2008). Constraints on lowermost mantle mineralogy and fabric beneath Siberia from seismic anisotropy. *Earth and Planetary Science Letters*, *275*(1–2), 32–42. https://doi.org/10.1016/j.epsl.2008.07.049

Wookey, J., Kendall, J.-M., & Rümpker, G. (2005). Lowermost mantle anisotropy beneath the north Pacific from differential S-ScS splitting. *Geophysical Journal International*, *161*(3), 829–838. https://doi.org/10.1111/j.1365-246X.2005.02623.x

Wysession, M. E., Langenhorst, A., Fouch, M. J., Fischer, K. M., Al-Eqabi, G. I., Shore, P. J., & Clarke, T. J. (1999). Lateral variations in compressional/shear velocities at the base of the mantle. *Science*, *284*(5411), 120–125. https://doi.org/10.1126/science.284.5411.120

Yang, F.-Q., Liu, B., Ni, S., Zeng, X., Dai, Z.-Y., & Lü, Y. (2008). Lowermost mantle shear velocity anisotropy beneath Siberia. *Acta Seismologica Sinica*, *21*(2), 213–216. https://doi.org/10.1007/s11589-008-0012-z

Zhu, H., Yang, J., & Li, X. (2020). Azimuthal anisotropy of the north American upper mantle based on full waveform inversion. *Journal of Geophysical Research: Solid Earth*, *125*(2), e2019JB018432. https://doi.org/10.1029/2019JB018432